Products and Kinetics of the Liquid-Phase Reaction of Glyoxal Catalyzed by Ammonium Ions (NH_4^+)

Barbara Nozière,*,† Pawel Dziedzic,‡ and Armando Córdova*,‡

Departments of Applied Environmental Sciences and Organic Chemistry, Stockholm University, SE-106 91 Stockholm, Sweden

Received: September 3, 2008; Revised Manuscript Received: November 6, 2008

Glyoxal, a common atmospheric gas, has been reported to be depleted in some regions of the atmosphere. The corresponding sink could be accounted for by reactions in or at the surface of atmospheric particles, but these reactions were not identified. Recently, we showed that inorganic ammonium ions, NH_4^+, are efficient catalysts for reactions of carbonyl compounds, including glyoxal, in the liquid phase. To determine whether ammonium-catalyzed reactions can contribute to depletion of glyoxal in the atmosphere, the reactivity of this compound in aqueous solutions containing ammonium salts (ammonium sulfate, chloride, fluoride, and phosphate) at 298 K has been studied. The products identified by LC-HRMS and UV absorption revealed a mechanism involving two distinct pathways: a Bronsted acid pathway and an iminium pathway. The kinetics of the iminium pathway was studied by monitoring formation of a specific product. This pathway was second order in glyoxal in most of the solutions studied and should therefore be second order in most ammonium-containing aerosols in the atmosphere. The corresponding rate constant, k^{II} (M^{-1} s^{-1}), increased strongly with ammonium ion activity, $a_{NH_4^+}$, and pH: k^{II} (M^{-1} s^{-1}) $= (2 \pm 1) \times 10^{-10}$ $\exp^{(1.5 \pm 0.8)a_{NH_4^+}}$ $\exp^{(2.5 \pm 0.2)pH}$. This iminium pathway is a lower limit for the ammonium-catalyzed consumption of glyoxal, but the contribution of the acid pathway is expected to be small in tropospheric aerosols. With these results the reactive uptake of glyoxal on ammonium-containing aerosols was estimated and shown to be a possible explanation for depletion of this compound in Mexico City.

Introduction

Glyoxal is a common gas in the atmosphere produced by oxidation of both biogenic and anthropogenic organic gases.[1] Development of new monitoring techniques for this compound has evidenced its contribution to the photochemical smog and, in particular, ozone concentration.[2] More recently, this compound was found to be at lower concentration than expected in the atmosphere of Mexico City.[3] This depletion was shown to be accounted for by either an uptake on atmospheric particles, an enhanced partitioning in the particulate aqueous phase, or an enhanced formation of secondary organic aerosols (SOA). However, in all these cases the chemical processes responsible for uptake or elevated partitioning were not identified. These observations suggest the existence of hitherto unknown chemical processes which would not only determine 70−95% of the atmospheric lifetime of glyoxal[3] but also affect the photochemistry and ozone budget and are therefore important to investigate. One of the explanations previously proposed for depletion of glyoxal was its reactive uptake by acidic aerosol particles.[3] In recent years, formation of secondary organic aerosols (SOA) was also shown to be enhanced by acid-catalyzed reactions.[4] However, calculations of the pH of inorganic aerosol particles in Mexico City with the model ISORROPIA,[5] validated by measurements of their ionic content,[6] led to values between 4 and 6, i.e., proton concentrations between $[H^+] = 10^{-6}$ and 10^{-4} M. Laboratory studies of the acid-catalyzed reactions of carbonyl compounds have established that these reactions or the partitioning of these compounds become significant for aerosols only for much larger acid concentrations, equivalent to at least 50 wt % of sulfuric acid ($[H^+] \approx 8.5$ M) and, in any case, $[H^+] \gg 1$ M.[7] Acid catalysis is thus unlikely to be responsible for depletion of glyoxal in the atmosphere. Our recent work identified several new classes of catalysts able to make reactions of carbonyl compounds as fast in tropospheric aerosols as in concentrated sulfuric acid.[8−10] The most important of them are probably inorganic ammonium ions, NH_4^+,[10] because of their ubiquitous presence and large concentrations in aerosols. A few studies of the uptake have reported glyoxal on sulfate particles, including ammonium sulfate ones.[11,12] However, they were based on measurements of particle growth, and could not clearly distinguish between reactive (or irreversible) and reversible uptake. For this reason and the large uncertainties on the Henry's law coefficient for glyoxal in these media these studies did not report any rate constant of reaction. Therefore, to obtain direct insight into the reactivity of glyoxal in ammonium-containing media we propose in this work to investigate its reactions directly in aqueous ammonium salts solutions (ammonium sulfate, ammonium chloride, ammonium fluoride, and ammonium phosphate) at room temperature, 298 ± 2 K. The first part of this work focuses on analyzing the reaction products and discussing the different pathways of the mechanism. The second part presents a kinetic study of one particular pathway, the iminium pathway, by monitoring formation of a specific product. Finally, the corresponding uptake of glyoxal on atmospheric particles is estimated and its importance for depletion of this compound in the atmosphere discussed.

* To whom correspondence should be addressed. E-mail: barbara.noziere@misu.su.se; acordova@organ.su.se.
† Department of Applied Environmental Sciences.
‡ Department of Organic Chemistry.

10.1021/jp8078293 CCC: $40.75
Published on Web 12/09/2008

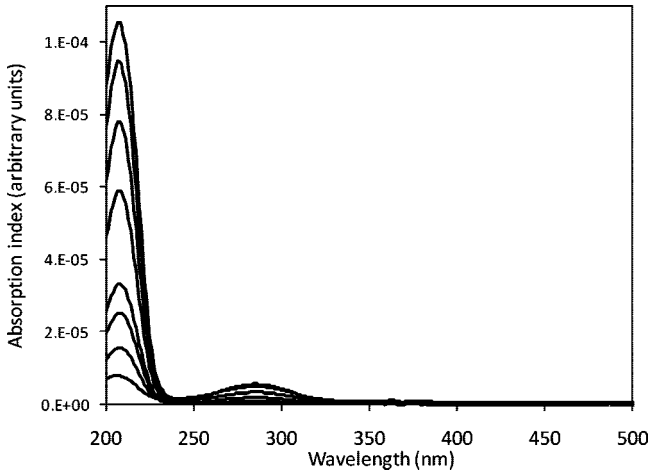

Figure 1. Absorption spectra the reaction of glyoxal (0.1 M) in ammonium sulfate 35 wt %, showing the rapid formation of a product at 209 nm.

Experimental Section

1. Product Study. The products of the ammonium-catalyzed reactions of glyoxal were identified by liquid chromatography−high-resolution mass spectrometry (HRMS) with a Bruker MicrOTOF spectrometer.

2. Kinetic Studies. The experimental technique and method used for the kinetic studies in this work are identical to those used in previous studies of amino acid catalysis,[8,9] and the reader is referred to these works for details. The experiments were performed on 4 mL bulk samples placed in glass vials, continuously stirred, and protected from light with aluminum foil at room temperature (298 ± 2 K). The solutions studied were mixtures of ammonium sulfate ($(NH_4)_2SO_4$), ammonium chloride (NH_4Cl), ammonium fluoride (NH_4F), and ammonium phosphate ($(NH_4)_2HPO_4$), 0.5−4 M in deionized water. Glyoxal, 0.05−1 M (generally 0.1 M), was introduced in these solutions with a microsyringe.

Kinetic analyses were based on measurements of the absorbance of the reaction mixtures as a function of time over 190−1100 nm with a UV−vis spectrometer (Agilent 8453) (see the example in Figure 1). For this small samples (<0.3 mL) of the reaction mixtures were taken and placed in 1 mm quartz cells. The absorbance of these samples, $A_b(\lambda)$, where λ is the wavelength in centimeters, measured by the spectrometer was converted into an extinction coefficient, ϵ_λ, by applying the Beer−Lambert law

$$A_b(\lambda) = \varepsilon_\lambda l \quad (1)$$

where l is the optical path length (l = 0.1 cm). For a direct comparison with the optical properties of atmospheric aerosols the absorbance presented in the figures was converted into absorption indices, A_λ (nondimensional), the imaginary part of the refraction index by

$$A_\lambda = \lambda\varepsilon_\lambda/4\pi \quad (2)$$

As discussed below, the kinetic studies in this work were based on absorption of a product at 209 nm (Figure 2). Using this absorption was reliable as no other products of the reaction studied were found to absorb light nor do products from the base- or acid-catalyzed reaction of glyoxal.

First-Order Analysis. The reactions were identified as being first order in glyoxal when the variations of the absorbance at 209 nm, $\epsilon_{209}(t)$, could be described with a first-order expression

$$\varepsilon_\lambda(t) = \varepsilon_\infty[1 - \exp(-k^I t)] \quad (3)$$

where ϵ_∞ is the absorbance of the mixture at long reaction time (or high degree of conversion), determined experimentally. The corresponding first-order rate constants, k^I (s^{-1}), were then determined from the slope of the expression

$$\ln(1-\varepsilon_\lambda/\varepsilon_\infty) = -k^I t \quad (4)$$

The overall uncertainties on these rate constants were estimated to about 25%.

Second-Order Analysis. As shown below, most of the reactions studied in this work followed second-order kinetics. This was established by fitting the variations of the absorption index at 209 nm with a second-order expression (Figure 2, top)

$$\varepsilon_{209}(t) = \varepsilon_\infty[1 - 1/(1 + C_\infty k^{II} t)] \quad (5)$$

where C_∞ (M) is the concentration of product at a high degree of conversion. The second-order rate constant, k^{II} (M^{-1} s^{-1}) was then obtained from the slope of the expression

$$[1/(1 - \varepsilon_{209}/\varepsilon_\infty)] - 1 = C_\infty k^{II} t \quad (6)$$

where C_∞ was calculated by dividing ϵ_∞ by the absorption cross-section of the product, σ(209 nm). The latter was assumed identical to the one of crotonaldehyde, σ(209 nm) = 37 150

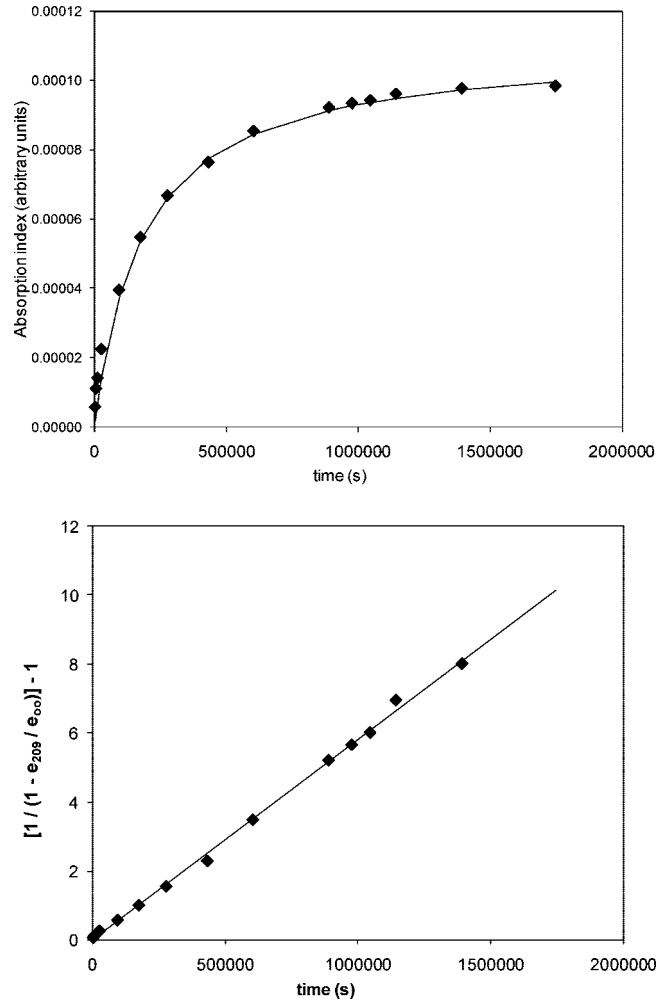

Figure 2. (Top) Real-time variations of the absorption index of the reaction mixture at 209 nm in saturated ammonium sulfate solutions (~43 wt %) and fit to the second-order function given by eq 5. (Bottom) Conversion of the real-time data into eq 6 to determine a second-order rate constant, k^{II} (M^{-1} s^{-1}) (see text).

TABLE 1: pH of the Solutions Used in the Kinetic Study and Activity Coefficients for the NH_4^+ Ions, $\gamma_{NH_4^+}$

solution	pH (±0.2)	$\gamma_{NH_4^+}$
$(NH_4)_2SO_4$ 20 wt % (1.6 M) n.b.[a]	5.5	0.43[c]
$(NH_4)_2SO_4$ 25 wt % (2) n.b.[a]	5.5	0.42[c]
$(NH_4)_2SO_4$ 30 wt % (2.6 M) n.b.[a]	5.5	0.43[c]
$(NH_4)_2SO_4$ 35 wt % (3 M) n.b.[a]	5.8	0.43[c]
$(NH_4)_2SO_4$ 40 wt % (3.5 M) n.b.[a]	5.5	0.45[c]
$(NH_4)_2SO_4$ satd[b] (43 wt %) n.b.[a]	4.9	0.46[c]
$(NH_4)_2SO_4$ 25% in buffer pH = 7	6.2	0.43
$(NH_4)_2SO_4$ 30% in buffer pH = 7	6.2	0.43
$(NH_4)_2SO_4$ 35% in buffer pH = 7	6.1	0.43
$(NH_4)_2SO_4$ 25% in buffer pH = 8	7.2	0.43
$(NH_4)_2SO_4$ 30% in buffer pH = 8	7.2	0.43
$(NH_4)_2SO_4$ 35% in buffer pH = 8	7.0	0.42
$(NH_4)_2SO_4$ 35% in buffer pH = 9	7.7	0.43
$(NH_4)_2SO_4$ 35% in buffer pH = 10	8.1	0.42
NH_4F 0.5 M, n.b.[a]	6.3	0.60
NH_4F 1 M, n.b.[a]	6.5	0.60
NH_4F 2 M, n.b.[a]	7.8	0.60
NH_4F 0.5 M in buffer pH = 7	6.7	0.60
NH_4F 0.5 M in buffer pH = 8	7.5	0.60
NH_4F 0.5 M in buffer pH = 9	8.1	0.60
$(NH_4)_2HPO_4$ 0.5 M	8.0	0.60
$(NH_4)_2HPO_4$ 1.33 M	8.2	0.59
NH_4Cl 2 M	4.8	0.61[c]
NH_4Cl 4 M	4.6	0.64[c]
NH_4Cl 4 M in buffer pH = 7	5.7	0.64[c]

[a] Nonbuffered. [b] Saturated. [c] From AIM model, ref 14.

M^{-1} cm^{-1}.[13] The overall uncertainties on k^{II} (M^{-1} s^{-1}) were estimated to be 50%. However, it is important to keep in mind that the absolute values of k^{II} reported in this work are inversely proportional to the value assumed for σ(209 nm). If better estimates for this cross-section become available these rate constants would have to be corrected accordingly.

Effect of Ammonium Ion Activity, Counterion, and pH. As the rate constant of reaction was expected to vary with the activity of the catalyst, experiments were carried out in salt concentrations varying from 0.5 to 4 M. The activities of NH_4^+, $a_{NH_4^+}$, in ammonium sulfate and ammonium chloride solutions were determined from the AIM model.[14] However, for ammonium fluoride or ammonium phosphate solutions, not included in the AIM model, the activity coefficients of ammonium ions, $\gamma_{NH_4^+}$, were assumed to be identical to those in diluted ammonium chloride solutions, $\gamma_{NH_4^+} = 0.60$. The activity coefficients of ammonium ions, $\gamma_{NH_4^+}$, attributed to the different solutions studied in this work are summarized in Table 1.

Our previous work on ammonium catalysis indicated that, for the same concentration of ammonium ions, different counterions result in different rate constants.[10] This effect is of first importance in the atmosphere because aerosols always contain mixtures of different salts. This was thus further investigated in this work by studying the reaction of glyoxal in as many different ammonium salt solutions as permitted by the experimental method: ammonium sulfate, ammonium fluoride, ammonium phosphate, and ammonium chloride. Unfortunately, ammonium nitrate and ammonium bromide solutions strongly absorb below 210 nm, precluding monitoring of the product at 209 nm, and were not studied in this work. Our previous work on amino acid catalysis suggested that the effect of different salts on the rate constant might be due to the basicity of the solutions rather than to ionic strength.[9] To investigate this series of experiments were performed where the pH of ammonium solutions was varied from about 5 (nonbuffered solutions) to 8 by adding buffers. The pHs of the different solutions studied are summarized in Table 1. "Blank" experiments were also performed in the buffer solutions alone (i.e., in the absence of ammonium salts) to ensure that no other reactions, in particular base-catalyzed ones, were interfering with the reaction studied. The activities of the ammonium ions in the buffered solutions were assumed identical to those in the nonbuffered ones (Table 1). In total, the kinetic study involved over a hundred experiments.

Chemicals. Glyoxal was 40% solution in water (~8.8 M), Aldrich. The salt solutions were prepared by mixing the salts with milliQ water: ammonium sulfate Sigma-Aldrich >99.0%; ammonium chloride Sigma, >99.5%; ammonium fluoride, Riedel de Haën, 98%; ammonium phosphate, Sigma-Aldrich, 98+%. Buffer solutions pH =7 (KH_2PO_4/Na_2HPO_4), 8 ($Na_2B_4O_7$/HCl), 9 ($Na_2B_4O_7$/HCl), and 10 ($Na_2B_4O_7$/NaOH), all Fixanal, Riedel de Haën.

Results and Discussion

1. Product Study. ***1.a. LC-HRMS Analyses.*** The products formed by the ammonium-catalyzed reaction of glyoxal were found to be mostly oligomeric species identical to those previously observed in the acid-catalyzed reaction of this compound[15] (see Table 2). These products can be explained by acid-catalyzed acetal formation and subsequent oligomerization[15] where the ammonium ions acted as a Bronsted acid and activated the glyoxal by protonation. However, some nitrogen-containing compounds not previously observed in acid catalysis were also found in this work, for instance, at $m/z = 192.0503$ (see Table 2). These products indicated the existence of an iminium pathway similar to the mechanism of amino acid catalysis.[9]

1.b. UV Absorption. Monitoring the reaction of glyoxal in ammonium salt solutions by UV−vis absorption in real time showed immediate formation of an absorption band at 209 nm (Figure 1). In some experiments, at long reaction time or high degree of conversion, a second absorption band appeared near 290 nm (also visible in Figure 1). Rapid formation of the band at 209 nm evidenced an irreversible step, while the slow build up of the band at 290 nm and its absence of further evolution indicated a product involved in an equilibrium or a reaction intermediate. Previous studies of the base- or acid-catalyzed reaction of glyoxal in the absence of ammonium ions (in sodium carbonate solutions, pH = 8−11,[10] or sulfuric acid[15]) did not report any product absorbing at 209 nm or susceptible to do so. This was also the case for the "blank" experiments performed in the buffer solutions (pH = 7−10) in this work. This confirmed the existence of an iminium pathway having a distinct mechanism from the base- and acid-catalyzed mechanisms and established that the product at 209 nm was specific to this pathway. The position and intensity of this absorption band suggested the $\pi \rightarrow \pi^*$ transition of a C=C or C=N bond. The second-order kinetics of this compound, presented below, implied that it was an oligomerization product. However, its rapid formation suggested a second-generation product or intermediate, i.e., involving two glyoxal molecules, rather than a third-generation product (involving three glyoxal molecules) such as the N-containing compound presented in Table 2.

2. Mechanism. The products found by HRMS analysis and UV absorption indicated that ammonium salts act as catalysts in two ways: by acting as a Bronsted acid (i.e., releasing protons) or forming covalent nitrogen species such as imminium intermediates (Scheme 1). Accordingly, in one pathway of this mechanism glyoxal is protonated by the ammonium salt and subsequently oligomerized by acetal (C−O bond) formation, as in the classical acid-catalyzed mechanism (Scheme 1A). In the other pathway the protonated glyoxal can undergo nucleophilic attack by ammonia followed by loss of water, giving the

TABLE 2: List of Product Masses Identified by HRMS, Their Relative Intensities, and Proposed Structures

Mass / relative intensity	Proposed structure
152.0556 / 11	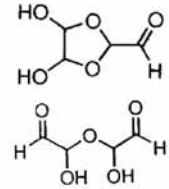
170.0651 / 90	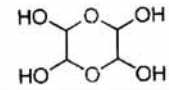
192.0496 / 580	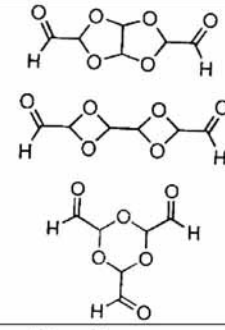
192.0503 / 190	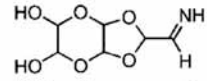
210.0610 / 25	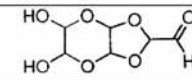
228.0706 / 160	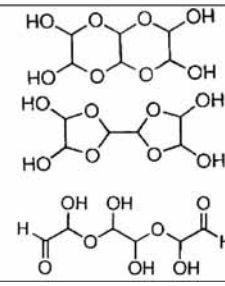

SCHEME 1: Main Pathways of the Reaction of Glyoxal Catalyzed by Ammonium Ions[a]

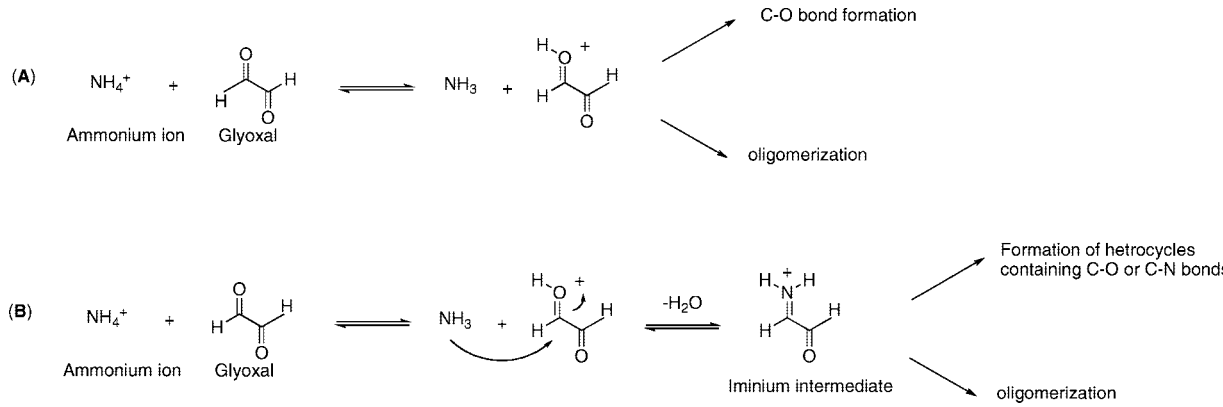

[a] The Bronsted acid pathway and iminium pathway (only the first steps of these pathways are shown).

corresponding iminium intermediate, which is activated for further transformations such as heterocyclic formation and oligomerization reactions (Scheme 1B).

3. Kinetic Study. As the compound absorbing at 209 nm was specific to the iminium pathway and no other product interfered with its absorption, monitoring its formation gave insight into the kinetics of the iminium pathway specifically. While this study had the advantage (over uptake experiments, for instance) of providing directly a rate constant of reaction, it is important to keep in mind that this pathway provides only a lower limit for the ammonium-catalyzed consumption of glyoxal.

In s 20 wt % ammonium sulfate solution formation of the product at 209 nm was first order in glyoxal and first-order analyses gave the rate constant $k^{I}(20\ \text{wt}\ \%) = (6.2 \pm 1.6) \times 10^{-6}\ \text{s}^{-1}$. In ammonium sulfate solutions 25 wt % and above as

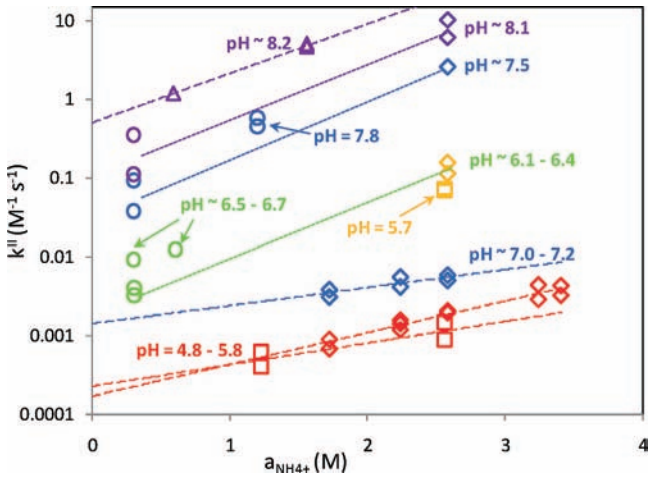

Figure 3. Second-order rate constant, k^{II} (M^{-1} s^{-1}), for the iminium pathway of the reaction of glyoxal in different ammonium salt solutions and pH conditions: Ammonium sulfate (diamonds), ammonium fluoride (circles), ammonium phosphate (triangles), and ammonium chloride (squares). Colors reflect the pH ranges: pH = 4.8−5.5 (red), 5.6−6 (yellow), 6.1−6.9 (green), 7.1−7.9 (blue), 8.0 and above (purple). Dashed lines: best fits to the data. Dotted lines: fit to eq 10 (see text).

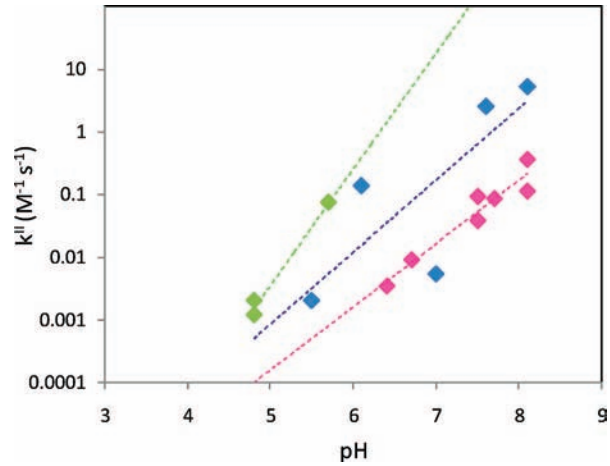

Figure 4. Effect of pH on the rate constant of the iminium pathway of the reaction of glyoxal, k^{II} (M^{-1} s^{-1}), in ammonium sulfate 35 wt % (blue), ammonium fluoride 0.5 M (pink), and ammonium chloride 4 M (green) solutions.

well as in all the other salt solutions studied (ammonium chloride, ammonium fluoride, and ammonium phosphate) formation of the product at 209 nm was second order in glyoxal (Figure 2). This implied that this iminium pathway should also be second order in most ammonium-containing aerosols in the atmosphere. Second-order analyses led to the corresponding second-order rate constants, k^{II} (M^{-1} s^{-1}), shown in Figure 3. For instance, k^{II} ($(NH_4)_2SO_4$, 25 wt %) = (8.0 ± 4.0) × 10^{-4} M^{-1} s^{-1}, $k^{II}(NH_4Cl, 2\ M)$ = (6.2 ± 2.0) × 10^{-4} M^{-1} s^{-1}, $k^{II}(NH_4F, 0.5\ M) = (3.7 \pm 2.0) \times 10^{-3}$ M^{-1} s^{-1}, $k^{II}((NH_4)_2HPO_4$, 0.5 M) = (1.2 ± 0.6) M^{-1} s^{-1}.

Transitions from first- to second-order kinetics were observed previously with amino acid catalysis[9] and indicated that first-order and second-order steps of the iminium pathway were in competition to limit formation of the product at 209 nm. The first-order step could be any of the steps depicted in Scheme 1A involving one glyoxal molecule, such as addition of ammonia for instance. However, as the oligomerization steps could not be elucidated, it was not possible to identify the second-order rate-limiting step.

Effect of Ammonium Ions Activity. As expected in catalysis, the second-order rate constant k^{II} (M^{-1} s^{-1}) increased with the activity of the ammonium ions, $a_{NH_4^+}$, in all solutions studied. Although this was difficult to interpret mechanistically, the variations of the rate constant were best described by exponential expressions. For instance, in nonbuffered solutions

$$k^{II}((NH_4)_2SO_4)(M^{-1}\ s^{-1}) = ((1.7 \pm 0.8) \times 10^{-4}) \exp^{(0.94 \pm 0.5) a_{NH_4^+}} \quad (7)$$

$$k^{II}(NH_4Cl)(M^{-1}\ s^{-1}) = ((2.0 \pm 1.0) \times 10^{-4}) \exp^{(0.74 \pm 0.5) a_{NH_4^+}} \quad (8)$$

$$k^{II}((NH_4)_2HPO_4)(M^{-1}\ s^{-1}) = (0.5 \pm 0.3) \exp^{(1.28 \pm 0.5) a_{NH_4^+}} \quad (9)$$

These expressions are represented by the dashed lines in Figure 3. The uncertainties quoted in eqs 7 and 8 reflect only the 50% uncertainties on each value of k^{II}. No expression is recommended for the rate constant in nonbuffered ammonium fluoride solutions because their pH varied significantly with concentration (see Table 1), which strongly affected the rate constant, as will be shown below. To a lower extent, the exponential factors in eqs 7 and 8 might also include some small effects due to slight variations of pH with concentration in these solutions.

Effect of Counterion and pH. The results in Figure 3 suggested that for the same concentration of ammonium ions different counterions result in different values of k^{II} with $k^{II}((NH_4)_2HPO_4) > k^{II}(NH_4F) > k^{II}((NH_4)_2SO_4) \approx k^{II}(NH_4Cl)$. Moreover, the results obtained at different pH but identical concentration of ammonium ions show that the rate constant, k^{II}, increases dramatically with pH in all salt solutions. Therefore, we examined if it was possible that the different values of k^{II} obtained with different counterions could be partly due to different pH. Indeed, it appeared that the expression

$$k^{II}(M^{-1}\ s^{-1}) = A \exp^{(1.5 \pm 0.8) a_{NH_4^+}} \quad (10)$$

could account well for the results both in nonbuffered solutions (eqs 7−9) and those obtained with different salts but at the same pH (for instance, between ammonium fluoride and ammonium sulfate at pH = 6.1/6.4, 7.5, and 8.1). These curves are represented by the dotted lines in Figure 3. Thus, within the uncertainties it seemed that the different rate constants obtained with different salts could mostly be attributed to different pH. This was an important result as it implied that k^{II} is entirely determined by only two parameters: $a_{NH_4^+}$ and pH (at a given temperature). The discrepancies between the exponential factors in eqs 7−9 and the one in eq 10 might be due to inaccurate assumptions for the activity coefficients of the ammonium ions, $\gamma_{NH_4^+}$, in some solutions (in particular in ammonium fluoride and phosphate).

The variations of k^{II} with pH for fixed concentrations of ammonium ions are reported in Figure 4 for ammonium sulfate, ammonium chloride, and ammonium fluoride solutions. These variations were very similar between the different solutions, with the exception of ammonium sulfate solutions at pH = 7, for which k^{II} was much lower than expected. The reasons for these discrepancies were not clear as low values of k^{II} were consistently obtained with all ammonium sulfate concentrations at pH = 7, which excluded the possibility of an experimental artifact. However, besides this exception, the variations of k^{II} as a function of pH in these different solutions could be summarized by a unique expression

$$k^{II}(M^{-1}\ s^{-1}) = f(a_{NH_4^+})\exp^{(2.5\pm1.0)pH} \quad (11)$$

where $f(a_{NH_4^+})$ are the variations of k^{II} with $a_{NH_4^+}$ described by eq 10. Note that the exponential expression as a function of pH is equivalent to a power expression of the concentration of protons: $\exp(2.5pH) = [H^+]^{-1.086}$. This strong and negative dependence of k^{II} with proton concentration might suggest that deprotonation is involved in the rate-limiting step.

Combining eqs 9 and 10 gave an expression allowing estimation of k^{II} in any aerosol composition (or other ammonium-containing media)

$$k^{II}(M^{-1}\ s^{-1}) = K\exp^{(1.5\pm0.8)a_{NH_4^+}}\ \exp^{(2.5\pm1.0)pH} \quad (12)$$

where $K = (2 \pm 1) \times 10^{-10}\ M^{-1}\ s^{-1}$ described best these results within the uncertainties introduced by eqs 10 and 11.

Although the kinetics of this iminium pathway is only a lower limit for the ammonium-catalyzed consumption of glyoxal, the rate constants reported for the acid-catalyzed reactions of carbonyl compounds[7] suggest that the contribution of the acid pathway should be small over the pH range studied in this work and relevant for tropospheric aerosols.

3. Atmospheric Implications. With eq 12 the rate of consumption of glyoxal in ammonium-containing particles in Mexico City can be estimated. While detailed calculations including the whole range of particle composition would have to be addressed by models, these simple calculations will assume a typical activity of $a_{NH_4^+} = 4$ M, representative of saturated ammonium sulfate particles and the dry conditions in Mexico City (RH = 50−85%).[3] For pH = 4 and 6 eq 12 gives $k^{II}_{NH_4}(pH = 4) = 2 \times 10^{-3}\ M^{-1}\ s^{-1}$ and $k^{II}_{NH_4}(pH = 6) = 0.26\ M^{-1}\ s^{-1}$. These second-order rate constants can be converted into apparent first-order ones by multiplying by the particulate concentration of glyoxal, X. Assuming that particulate glyoxal is in equilibrium with the gas, $X = RTHC$, where R is the gas constant, T the temperature, H its apparent Henry's law coefficient, and C its gas-phase concentration. For $C =$ 1 ppb V[3] and H identical as in seawater, $H = 3.6 \times 10^5\ M\ atm^{-1}$,[16] $X = 3.5 \times 10^{-4}$ M, and the apparent first-order decay of glyoxal due to ammonium-catalyzed reaction in particles would be between $k^{I}_{NH_4}(pH = 4) = 7 \times 10^{-7}\ s^{-1}$ and $k^{I}_{NH_4}(pH = 6) = 9 \times 10^{-5}\ s^{-1}$.

These rates can be compared with those of other possible reactions of glyoxal in particles, in particular with OH radicals. The rate constant for reaction of glyoxal with OH radicals in aqueous solutions is $k^{II}_{OH} = 10^9\ M^{-1}\ s^{-1}$.[17] The concentration of OH radicals in particles is not known, but upper limits are given by the concentrations calculated for cloud droplets, [OH] = 10^{-15}−10^{-13} M,[18,19] where less reactants are present to consume OH radicals and at lower concentrations than in aerosol particles. These concentrations correspond to $k^{I}_{OH} = 10^{-6}$−10^{-4} s^{-1}, which is on the same order as the first-order decays for the ammonium-catalyzed reaction. Thus, while ammonium catalysis might be the main sink for glyoxal at night, the reaction with OH radicals would be an additional sink, potentially of the same magnitude, during daylight.

The first-order rates constants, $k^{I}_{NH_4}$, allow calculation of the corresponding uptake

$$\gamma_r = \frac{4RTH\sqrt{k^{I}_{NH_4}D}}{\omega} \quad (13)$$

where ω is the molecular speed of glyoxal, $\omega \approx 3.3 \times 10^4$ cm s^{-1}, and D its diffusion coefficient, estimated to 5×10^{-7} cm^2 s^{-1} in supersaturated ammonium sulfate particles.[20] Equation 13 thus leads to $\gamma_r = 0.6 \times 10^{-3}$ to 7×10^{-3} for particles between pH = 4 and 6. This range contains the uptake value previously estimated to account for depletion of glyoxal in Mexico City, $\gamma_r = 3.7 \times 10^{-3}$,[3] suggesting that the ammonium-catalyzed reaction of glyoxal in aerosols is a possible explanation for this depletion.

However, for fine particles the effective uptake might not be as large as that estimated above if glyoxal is not consumed fast enough in the particles.[21] This effect can be accounted for by a correction factor, c, such as $\gamma_{eff} = \gamma_r c$, where $c = r/(3l)$ and l is the diffuso-reactive length (distance over which the reaction is taking place in the particles), given by[21]

$$l = \sqrt{\frac{D}{k^{I}_{NH_4}}} \quad (14)$$

Thus, for particles of a radius $r = 500$ nm, $c(pH = 4) = 1.4 \times 10$ and $c(pH = 6) = 2 \times 10$, and γ_{eff} would not be large enough to explain depletion of glyoxal in Mexico City.

Another factor, however, might further increase this uptake: the apparent Henry's law coefficient, H. As previously evidenced in acid catalysis, catalysis increases not only the rate constants of (irreversible) reactions but also the apparent Henry's law coefficient for the reactant because (reversible) equilibria occurring in the reactive system allow more molecules of reactant to be stabilized in solution. This effect is not taken into account in eq 13 unless an apparent Henry's law coefficient is used. For instance, the apparent Henry's law coefficients for acetaldehyde, acetone, and other carbonyl compounds were shown to increase by about a factor 40 between 50 and 90 wt % H_2SO_4.[7b] The Henry's law coefficient of glyoxal might thus also be larger in ammonium-containing particles than in water. Large Henry's law coefficients for glyoxal were actually reported from smog chamber experiments, $H = 2.6 \times 10^7$ M atm^{-1},[12] and $H_{eff} = 4 \times 10^9\ M\ atm^{-1}$ was found to account for its depletion in Mexico City.[3] In both cases, the values are likely to be upper limits of the actual coefficient as the sinks they account for might contain both reversible and irreversible components. However, using $H = 2.6 \times 10^7\ M\ atm^{-1}$ leads to an effective uptake of glyoxal (i.e., including the correction for small particles) between $\gamma_{eff} = 0.07 \times 10^{-3}$ and 8.5×10^{-3} for particles between pH = 4 and 6, which would account for depletion of glyoxal.

Finally, it is also possible that the ammonium-catalyzed reaction of glyoxal leads not only to the uptake of this compound but also to formation of SOA, as observed with acid catalysis.[4] In this case, the sink for glyoxal cannot be estimated only by an irreversible uptake or only by reversible partitioning into particles but by a combination of both. In particular, the correction factor on the uptake coefficient discussed above would not apply as fine particles would not saturate but grow in size. However, calculation of the sink of glyoxal resulting from such processes is complex and would have to be addressed by models.

Conclusion

In this work the reactivity of glyoxal catalyzed by ammonium ions was investigated directly in aqueous ammonium salt solutions. The occurrence of an irreversible reaction in these solutions, which could not be conclusively established by previous uptake studies, was confirmed. Product analyses evidenced a mechanism proceeding by two pathways: a Bronsted acid pathway where the protons are provided by the ammonium ions and the products identical to those obtained with strong

acids and an iminium pathway producing N-containing products and intermediates.

The iminium pathway was second order in glyoxal in most the solutions studied and should therefore be second order in most ammonium-containing aerosols in the atmosphere. The corresponding rate constant, k^{II} (M^{-1} s^{-1}), increased strongly with ammonium ion activity, $a_{NH_4^+}$, and pH. This effect of pH largely accounted for the different rate constants obtained with different salts, and an expression for k^{II} was proposed to estimate this rate constant in any aerosol composition as a function of only two parameters, $a_{NH_4^+}$ and pH. We emphasize, however, that the values for k^{II} reported in this work depend directly on the absorption cross-section assumed for the product at 209 nm and should be corrected if better estimates become available. With these results, the ammonium-catalyzed consumption of glyoxal by aerosol particles in Mexico City was estimated and shown to be a possible explanation for its depletion depending on the value of its Henry's law coefficient and type of process taking place (reactive uptake only or reactive uptake/SOA formation). A detailed treatment of these processes, including the full range of aerosol size and composition, would now be necessary to obtain a definitive answer. In addition, the uptake estimated in this work is likely to be a lower limit of actual ones as the Bronsted acid pathway of the ammonium-catalyzed reaction, expected to be small but perhaps not negligible at pH < 5, was not taken into account. Other reactions, in particular with OH radicals, might also contribute significantly to the sink of glyoxal in aerosols during daylight. However, in general, the results of this work confirm the potential importance of ammonium catalysis in atmospheric aerosols.

Acknowledgment. B.N. acknowledges support of a Marie Curie Chair from the European Commission. A.C. acknowledges support from the Swedish National Research Council.

References and Notes

(1) Fu, T. M.; Jacob, D. J.; Wittrock, F.; Burrows, J. P.; Vrekoussis, M.; Henze, D. K *J. Geophys. Res.* **2008**, 113; D15303, doi:10.1029/2007JD009505.

(2) Volkamer, R.; Molina, L. T.; Molina, M. J.; Shirley, T.; Brune, W. H. *Geophys. Res. Lett.* **2005**, 32; L08806, doi:10.1029/2005GL022616.

(3) Volkamer, R.; San Martini, F.; Molina, L. T.; Salcedo, D.; Jimenez, J. L.; Molina, M. J. *Geophys. Res. Lett.* **2007**, 34; L19807, doi:10.1029/2007GL030752.

(4) Jang, M.; Czoschke, N. M.; Lee, S.; Kamens, R. M. *Science* **2002**, *298*, 814.

(5) San Martini, F. M.; Dunlea, E. J.; Volkamer, R.; Onasch, T. B.; Jayne, J. T.; Canagaratna, M. R.; Worsnop, D. R.; Kolb, C. E.; Shorter, J. H.; Herndon, S. C.; Zahniser, M. S.; Salcedo, D.; Dzepina, K.; Jimenez, J. L.; Ortega, J. M.; Johnson, K. S.; McRae, G. J.; Molina, L. T.; Molina, M. J. *Atmos. Chem. Phys.* **2006**, *6*, 4889–4904.

(6) Salcedo, D.; Onasch, T. B.; Dzepina, K.; Canagaratna, M. R.; Zhang, Q.; Huffman, J. A.; DeCarlo, P. F.; Jayne, J. T.; Mortimer, P.; Worsnop, D. R.; Kolb, C. E.; Johnson, K. S.; Zuberi, B.; Marr, L. C.; Volkamer, R.; Molina, L. T.; Molina, M. J.; Cardenas, B.; Bernabé, R. M.; Márquez, C.; Gaffney, J. S.; Marley, N. A.; Laskin, A.; Shutthanandan, V.; Xie, Y.; Brune, W.; Lesher, R.; Shirley, T.; Jimenez, J. L. *Atmos. Chem. Phys.* **2006**, *6*, 925.

(7) (a) Baigrie, L. M.; Cox, R. A.; Slebocka-Tilk, H.; Tencer, M.; Tidwell, T. *J. Am. Chem. Soc.* **1985**, *107*, 3640. (b) Esteve, W.; Nozière, B. *J. Phys. Chem. A* **2005**, *109*, 10920. (c) Casale, M. T.; Richman, A. R.; Elrod, M. J.; Garland, R. M.; Beaver, M. R.; Tolbert, M. A. *Atmos. Environ.* **2007**, *41*, 6212.

(8) Nozière, B.; Dziedzic, P.; Córdova, A. *Geophys. Res. Lett.* **2007**, 34; L21812, doi:10.1029/2007GL031300.

(9) Nozière, B.; Córdova, A. *J. Phys. Chem. A* **2008**, *112*, 2827.

(10) (a) Nozière, B., Córdova, A. International Patent Application P08040PC, Oct. 2, 2007. (b) Nozière, B., Dziedzic, P. Córdova, A. *Atmos. Chem. Phys. Discuss.* **2008**.

(11) Liggio, J.; Li, S.-M.; McLaren, R. *J. Geophys. Res.* **2005**, *110*, D10304, doi: 10.1029/2004JD005113.

(12) Kroll, J. H.; Ng, N. L.; Murphy, S. M.; Varutbangkul, V.; Flagan, R. C.; Seinfeld, J. H *J. Geophys. Res* **2005**, *110*, D23207; doi:10.1029/2005JD006004.

(13) Blout, E. R.; Fields, M. *J. Am. Chem. Soc.* **1948**, *70*, 189.

(14) Clegg, S. L.; Brimblecombe, P.; Wexler, A. S. *J. Phys. Chem. A* **1998**, *102*, 2155.

(15) Liggio, J.; Li, S.-M.; McLaren, R. *Environ. Sci. Technol.* **2005**, *39*, 1532.

(16) Zhou, X.; Mopper, K. *Environ. Sci. Technol.* **1990**, *24*, 1864.

(17) Buxton, G. V.; Malone, T. N.; Salmon, G. A. *J. Chem. Soc., Faraday Trans.* **1997**, *93*, 2889.

(18) Herrmann, H.; Ervens, B.; Jacobi, H.-W.; Wolke, R.; Nowacki, P.; Zellner, R. *J. Atmos. Chem.* **2000**, *36*, 231.

(19) Lim, H.-J.; Carlton, A. G.; Turpin, B. J. *Environ. Sci. Technol.* **2005**, *39*, 4441.

(20) Easteal, A. J.; Woolf, L. A. *J. Sol. Chem.* **1996**, *25*, 937.

(21) Hanson, D. R.; Ravishankara, A. R.; Solomon, S. *J. Geophys. Res.* **1994**, *99*, 3615.

JP8078293